Journal of Visualized Experiments

In vivo quantification of protein turnover in aging C. elegans using the photoconvertable Dendra2

--Manuscript Draft--

Article Type:	Invited Methods Collection - JoVE Produced Video
Manuscript Number:	JoVE61196R2
Full Title:	In vivo quantification of protein turnover in aging C. elegans using the photoconvertable Dendra2
Keywords:	C. elegans, Huntingtin, Proteostasis Network, Degradation, Dendra2, Photoconversion, Confocal microscopy, Fiji/ImageJ.
Corresponding Author:	Janine Kirstein Universitat Bremen Bremen, Bremen GERMANY
Corresponding Author's Institution:	Universitat Bremen
Corresponding Author E-Mail:	kirstein@uni-bremen.de
Order of Authors:	Maria Lucia Pigazzini
	Janine Kirstein
Additional Information:	
Question	**Response**
Please indicate whether this article will be Standard Access or Open Access.	Standard Access (US$2,400)
Please indicate the **city, state/province, and country** where this article will be **filmed**. Please do not use abbreviations.	Berlin, Germany

TITLE:

In Vivo Quantification of Protein Turnover in Aging *C. elegans* using Photoconvertible Dendra2

AUTHORS AND AFFILIATIONS:

Maria Lucia Pigazzini[1,2], Janine Kirstein[1,3]

[1]Leibniz Research Institute for Molecular Pharmacology im Forschungsverbund, Berlin, Germany
[2]NeuroCure Cluster of Excellence, Charité – Universitätsmedizin Berlin, Germany
[3]Department of Biology and Chemistry, University of Bremen, Bremen, Germany

Corresponding Author:

Janine Kirstein (kirstein@uni-bremen.de)

Email Address of Co-author:

Maria Lucia Pigazzini (pigazzini@fmp-berlin.de)

KEYWORDS:

C. elegans, huntingtin, proteostasis network, degradation, Dendra2, photoconversion, confocal microscopy, Fiji/ImageJ

SUMMARY:

Presented here is a protocol to monitor degradation of the protein huntingtin fused to the photoconvertible fluorophore Dendra2.

ABSTRACT:

Proteins are synthesized and degraded constantly within a cell to maintain homeostasis. Being able to monitor the degradation of a protein of interest is key to understanding not only its life cycle, but also to uncover imbalances in the proteostasis network. This method shows how to track the degradation of the disease-causing protein huntingtin. Two versions of huntingtin fused to Dendra2 are expressed in the *C. elegans* nervous system: a normal version or one with an expanded and pathogenic stretch of glutamines. Dendra2 is a photoconvertible fluorescent protein; upon a short ultraviolet (UV) irradiation pulse, Dendra2 switches its excitation/emission spectra from green to red. Similar to a pulse-chase experiment, the turnover of the converted red-Dendra2 can be monitored and quantified, regardless of the interference from newly synthesized green-Dendra2. Using confocal-based microscopy and due to the optical transparency of *C. elegans,* it is possible to monitor and quantify the degradation of huntingtin-Dendra2 in a living, aging organism. Neuronal huntingtin-Dendra2 is partially degraded soon after conversion and cleared further over time. The systems controlling degradation are deficient in the presence of mutant huntingtin and are further impaired with aging. Neuronal subtypes within the same nervous system exhibit different turnover capacities for huntingtin-Dendra2. Overall, monitoring any protein of interest fused to Dendra2 can provide important information not only on its degradation and the players of the proteostasis network involved, but also on its location, trafficking, and transport.

INTRODUCTION:

The proteome of a living organism is constantly renewing itself. Proteins are continuously degraded and synthesized according to the physiological demand of a cell. Some proteins are quickly eliminated, whereas others are longer lived. Monitoring protein dynamics is a simpler, more accurate, and less invasive task when using genetically encoded fluorescent proteins (FPs). FPs form autocatalytically and can be fused to any protein of interest (POI), but do not require enzymes to fold or need cofactors save for oxygen[1]. A newer generation of FPs has recently been engineered to switch color upon irradiation with a light pulse of determined wavelength. These photoactivatable FPs (PAFPs) allow for labeling and tracking of POIs, or the organelles or cells they reside in, and examine quantitative and/or qualitative parameters[2]. FPs make it possible to track any POI's movement, directionality, rate of locomotion, coefficient of diffusion, mobile versus immobile fractions, the time it resides in one cellular compartment, as well as its turnover rate. For specific organelles, locomotion and transport, or fission and fusion events can be determined. For a particular cell type, a cell's position, rate of division, volume, and shape can be established. Crucially, the use of PAFPs allows tracking without continuous visualization and without interference from any newly synthetized probe. Studies both in cells and in whole organisms have successfully employed PAFPs to address biological questions in vivo, such as the development of cancer and metastasis, assembly or disassembly of the cytoskeleton, and RNA-DNA/protein interactions[3]. In this manuscript, light microscopy and PAFPs are used to uncover the turnover rates of the aggregation-prone protein huntingtin (HTT) in vivo in a *C. elegans* model of neurodegenerative disease.

The protocol described here quantifies the stability and degradation of the fusion protein huntingtin-Dendra2 (HTT-D2). Dendra2 is a second-generation monomeric PAFP[4] that irreversibly switches its emission/excitation spectra from green to red in response to either UV or visible blue light, with an increase in its intensity of up to 4,000-fold[5,6]. Huntingtin is the protein responsible for causing Huntington's disease (HD), a fatal hereditary neurodegenerative disorder. Huntingtin exon-1 contains a stretch of glutamines (CAG, Q). When the protein is expressed with over 39Q, it misfolds into a mutant, toxic, and pathogenic protein. Mutant HTT is prone to aggregation and leads to neuronal cell death and degeneration, either as a short oligomeric species or as larger highly structured amyloids[7].

The nematode is a model system for studying aging and neurodegeneration thanks to its ease of manipulation, isogenic nature, short lifespan, and its optical transparency[8]. To study the stability of HTT in vivo, a fusion construct was expressed in the nervous system of *C. elegans*. A HTT-D2 transgene containing either a physiological stretch of 25Qs (HTTQ25-D2) or a pathological stretch of 97Qs (HTTQ97-D2) is overexpressed pan-neuronally throughout the nematode´s lifetime[9]. By subjecting live *C. elegans* to a brief and focused point of light, a single neuron is photoswitched and the converted HTT-D2 is tracked over time. To establish the amount of HTT-D2 degraded, the difference between the red signal of the freshly converted HTT-D2 is compared to the remaining red signal of HTT-D2 after a determined period of time. Therefore, it becomes possible to investigate how huntingtin is degraded when found in its expanded and toxic form compared to its physiological form; how anterior or posterior neurons respond differently to the presence

of Q97 versus Q25, especially over prolonged time periods; and how the collapse of the proteostasis network (PN) during aging contribute to the differences in degradation rates. These results only describe a small set of observations on the turnover of HTT-D2. However, many more biological questions relevant to both the field of protein aggregation and proteostasis can be addressed with this in vivo application.

PROTOCOL:

1. Generation of *C. elegans* expressing neuronal Huntingtin-Dendra2 fusion protein

1.1. Clone the gene encoding the POI in a nematode expression vector (i.e., pPD95_75, Addgene #1494), by traditional restriction enzyme digest[10], Gibson assembly[11], or any method of choice. Insert a promoter to drive expression in a desired tissue or at a desired developmental stage. Insert the Dendra2 fluorophore either N- or C-terminally in frame with the POI.

1.2. Generate transgenic *C. elegans* expressing the fusion construct (e.g., via microinjection)[12].

NOTE: The plasmid carrying the transgene will remain as an extrachromosomal array. Integration of the construct is not necessary but can be performed if desired[13]. In this protocol, *C. elegans* were microinjected with a plasmid carrying the fusion construct huntingtin exon 1-Dendra2 (HTT-D2) under the control of the pan-neuronal promoter *prgef-1*. The *C. elegans* expression backbone was obtained from Kreis et al.[14], the huntingtin exon 1 with either Q25 or Q97 was obtained from Juenemann et al.[15], and Dendra2 was obtained from Hamer et al.[16].

2. Age matching and maintenance of *C. elegans*

2.1. Age match all nematodes by synchronizing either with alkaline hypochlorite solution treatment[17] or via egg laying for 4 h at 20 °C. For egg laying, place 10 gravid adults on a freshly seeded NGM plate and leave for 4 h before removing. The eggs laid in this timespan will give rise to synchronized nematodes.

2.2. Keep experimental *C. elegans* on nematode growth media (NGM) plates seeded with the bacterial food source *E. coli* OP50, following standard nematode husbandry[18].

2.3. Grow nematodes at 20 °C to the desired stage. For this protocol, the required ages are days 4 and 10.

NOTE: Young adults at day 4 can be identified by the presence of eggs in their gonads and their high mobility. Aged day 10 nematodes are post-fertile, and undergo tissue deterioration and locomotive decline[19].

2.4. For day 10 nematodes, passage daily after the L4 stage at day 3, once nematodes are fertile, to avoid a mixed population.

3. Preparation of microscopy slides for imaging

3.1. Prepare the microscopy slides on the day of imaging. In a microwave, melt general grade agarose at a concentration of 3% (w/v) in ddH_2O. Leave to cool slightly.

3.2. Cut the tip of a 1 mL pipette tip and aspirate roughly 400 µL of melted agarose. Gently place a few drops of agarose onto a clean glass slide and immediately place another slide on top, making sure that a thin pad of agarose is created between the two. Let dry before gently sliding or lifting the top slide off.

3.3. Place the agarose pad slides in a humidified container to prevent them from drying out. These can be used within 2–3 h.

NOTE: Avoid formation of small bubbles in the agarose, as the nematodes can be trapped within.

4. Definition of confocal microscope parameters

NOTE: Before mounting the nematodes and data acquisition, define all settings on the confocal acquisition software. The settings can be adapted to the imaging hardware and software of choice.

4.1. Open the confocal software and define the laser imaging settings. Set the light path for excitation/emission for green Dendra2 at 486–553 nm and for red Dendra2 at 580–740 nm. Adjust the power and gain of both channels/lasers according to the intensity of the fluorophore. Do not change the digital gain or offset and set the pinhole as fully open.

4.2. Define the acquisition setup: select a sequential channel mode and switch track every frame. Set the scan mode as frame, and the frame size as 1,024 x 1,024, with a line step of 1. Set the averaging to 2, and average by mean method and mode of unidirectional line. Set the bit depth to 8 bits.

4.3. Define the multidimensional acquisitions settings for the conversion of Dendra2. For conversion and bleaching use the 405 nm diode laser set at 60% energy power. If available, activate the safe bleaching GaAsP to protect the detectors.

4.4. Select a time series of two cycles, with a 0.0 ms interval in between, and normal start and stop. Start bleaching after scan 1 of 2 and repeat for 30 iterations. Stop bleaching when the intensity drops to 50%.

4.5. Define the speed of acquisition/pixel dwell as fast (e.g., maximum = 12) for conversion, and medium speed (e.g., medium = 5) for capturing a snap image.

NOTE: The bleaching parameters defined here are guidelines. For other Dendra2 tagged POIs the laser power settings and bleaching iterations and values must be established empirically.

5. Mounting of *C. elegans* onto microscopy slides

NOTE: If possible, place a mounting stereomicroscope close to the confocal microscope setup and mount the nematodes just before imaging.

5.1. On the glass cover slide on the opposite side of the agarose pad, draw a window with four squares with a permanent marker and number them.

5.2. Pipette 15 µL of levamisole in the middle of the agarose pad. The concentration of levamisole will vary according to the nematode´s age: When imaging day 4 nematodes use 2 mM levamisole; when imaging day 10 nematodes use 0.5 mM levamisole.

5.3. Transfer four nematodes into the liquid using a wire pick. With the help of an eyelash pick, gently move each individual nematode to a window square. Swivel the eyelash so that any trace of *E. coli* OP50 is diluted and its fluorescent background does not interfere with signal acquisition.

5.4. Wait for the nematodes to almost stop moving and gently place a cover slip on top of the liquid to immobilize the nematodes in the layer of levamisole between the agarose pad and the cover slip.

5.5. Place the inverted slide on the confocal stage to image the nematodes.

6. Conversion of green Dendra2: Data acquisition at time zero

NOTE: The pulse-chase experiments start by irreversibly converting the Dendra2 fusion protein from a green emitting fluorophore to a red one.

6.1. Using the microscope´s eyepiece, locate the first nematode with a 20x objective under green fluorescence. Focus on the head or tail and switch to confocal mode.

6.2. Start live laser scanning with the 488 nm blue laser to visualize the green Dendra2 in the EGFP green channel (ex/em = 486–553 nm). Select a single neuron and bring it into focus. Zoom in 3x and increase the target of the laser beam[4].

NOTE: Select one neuron per nematode. Each neuron will constitute one sample or data point.

6.3. Find the maximum projection plane and, according to the brightness of the fluorophore, increase or decrease the gain or laser power to obtain a saturated but not overexposed image identifiable by the color range indicator. Once this is defined, stop the scanning.

NOTE: Do not irradiate the sample for too long or with too much power, as excitation with visible blue 488 nm light can also convert Dendra2, albeit slowly and less efficiently[4].

6.4. In the software, open the tab to select the regions of interest (ROIs) and draw a first ROI around the selected neuron. Define a larger second region of interest encompassing the nematode´s head and including the first ROI.

6.5. In the bleaching settings, select for the first ROI to be acquired, bleached, and analyzed. Select for the second ROI to be acquired and analyzed but not bleached.

6.6. Set the speed of scanning to maximum (i.e., fast pixel dwell) and start the experiment to convert the selected Dendra2 neurons.

NOTE: Once the experiment is done the acquired picture will result in two images: one before and one after conversion. For the green channel, the first image should have a higher green signal that diminishes in the second image due to the conversion of the green Dendra2. For the red channel, the first image should be negative and show no signal, with a red signal appearing in the after conversion image. If the green signal does not diminish, the conversion did not occur, and the settings, such as the 405 laser power or the number of iterations, should be modified. If there is a red signal in the first image, then the 488 nm laser power used was too high and a portion of the green Dendra2 was already converted to red. In this case, a new neuron/nematode should be selected.

6.7. Immediately after conversion, start live scanning with the green 561 nm laser to visualize Dendra2 in the red channel (ex/em = 580–740 nm). Find the focus and respective maximum projection of the converted neuron using the range color indicator to avoid overexposure.

6.8. Quickly set the scan rate to a lower pixel dwell speed (e.g., 5x) and acquire a snapshot image of both channels at a higher resolution. This image is defined as timepoint zero (T0) after conversion.

NOTE: The speed of acquisition for the converted image can be varied. However, once chosen, this speed needs to stay constant throughout the data collection.

6.9. Save the scan with an identifiable name and/or number, followed by the time zero label (T0).

NOTE: It is advisable to also save the image of the conversion experiment (step 6.6) to illustrate the lack of red signal before conversion and its appearance afterwards.

7. Imaging of converted red Dendra2 for data acquisition at a selected second time point

7.1. To track Dendra2 degradation over time, define a second timepoint to reimage the same nematode/neuron. Select the second timepoint experimentally to address any relevant biological question. For the protocol described here, Dendra2 is imaged both at 2 h (T2) and 24 h (T24) post conversion.

7.1.1. At the selected timepoint, find the same nematode/neuron with the use of the eyepiece

and red fluorescence.

7.1.2. Open the T0 image of the respective nematode/neuron and reload/reuse the image settings. Ensure that the acquisition settings of the snapshot are precisely the same when acquiring the T0, T2, and T24 h images.

7.1.3. Scanning live in the red channel, bring the converted red neuron into focus. Because the red Dendra2 degrades over time the range indicator will show a less intense maximum projection. Do not change any acquisition parameters and obtain a snapshot at the same speed (e.g., 5x) as the first image.

7.2. To track the degradation of Dendra2 after 4 h or longer, rescue the nematodes after conversion.

7.2.1. Remove the slide from the microscope immediately after converting and imaging the four nematodes. Gently remove the coverslip and with the use of a wire pick, lift each nematode from the agarose pad.

7.2.2. Place each nematode individually on an appropriately labelled and identifiable NGM plate.

7.2.3. For the second time point, mount the nematode again onto a fresh agarose pad and proceed with the imaging of the converted red Dendra2 following the instructions in section 6.

8. Image analysis of converted Dendra2

NOTE: Analysis of the degradation of Dendra2 is performed with Fiji/ImageJ software[20].

8.1. Open Fiji and drag and drop the .lsm file into the Fiji bar. Open the T0 image taken just after conversion and the image of the same nematode taken at the selected time point after conversion (T2 or T24 h).

NOTE: To track the degradation of the protein of interest fused to Dendra2 only the red channel needs to be analyzed.

8.2. Establish the measurement parameters from the menu: **Analyze | Set Measurements.** Select the **Area** and **Integrated Density** functions.

8.3. Select the image obtained with the red channel. Select the **Polygon Selection Tool** from the Fiji bar.

8.4. Identify the converted neuron on the T0 image and draw an ROI around it using the selection tool.

8.4.1. To properly identify the contours of the neuron, highlight the intensity thresholds by

selecting from the bar **Image | Adjust | Threshold.** Drag the bar cursor to delineate the threshold and track around this area with the polygon tool. To generate an accurate ROI, it is also possible to use the contour of the selected neuron from the green channel.

8.5. Once the selection has been made in the red channel window, press **Analyze | Measure**. A pop-up window named **Results** will appear and include the ROI values for **Area, IntDen**, and **RawIntDen**.

8.6. Perform the same process of selection and measurement for the image of the second time point (T2 or T24 h).

8.7. Copy the obtained values into a spreadsheet software, taking care to appropriately record the values at T0 after conversion, and at T2 or T24 h after conversion.

9. Calculating the ratio of Dendra2 degradation

9.1. To calculate the ratio of degradation, first assign a value of 1 (or 100%) to time the degradation from time point zero (i.e., just after conversion, when all of the red Dendra2 converted is still present). This results from dividing the value of IntRawDen of T0 by itself.

9.2. To calculate the reduction of the red Dendra2 intensity signal over time, and the degradation, divide the value of **RawIntDen** of the second time point (e.g., T2 or T24 h) by the value of the **RawIntDen** of T0. The resulting number should be less than 1. These values can also be expressed as percentages, defining T0 as 100%.

9.3. Repeat section 7 for each nematode converted. For a graphical representation of the degradation of Dendra2, chart a scatter plot or bar graph with the percentage or ratio values of fluorescence decrease obtained in the y axis. Apply any desired statistical analysis and illustrate it on the graph.

REPRESENTATIVE RESULTS:

Two nematode strains expressing the huntingtin exon-1 protein fragment in frame with the photoconvertible protein Dendra2 were obtained via microinjection and the plasmids were kept as an extrachromosomal array. The fusion construct was expressed in the whole *C. elegans* nervous system from development throughout aging. Here, HTT-D2 contained either the physiological 25 polyglutamine stretch (HTTQ25-D2, **Figure 1A**) or a fully penetrant and pathogenic repeat with 97 glutamines (HTTQ97-D2, **Figure 1B**). Initially the fusion protein was tested to make sure it changed from its green spectrum to its red spectrum upon UV irradiation. HTT-D2 successfully switched from green to red exclusively within the illuminated region. According to the power and iterations of the UV pulse, and depending on the z-plane and penetrance of the laser beam through the cuticle of the nematode, a defined portion of HTT-D2 was converted, but not all. A red signal appeared within the photoconverted neurons, colocalizing with the green nonconverted HTT-D2 (**Figure 1C,D**). Due to the accuracy of the laser scanning photon beams it was possible to convert a precise ROI corresponding to a single neuron.

Before conversion, no red signal was visible when the sample was excited in the red channel (**Figure 2A**). Upon UV irradiation, the green signal diminished as HTT-D2 was converted and a red signal finally appeared (**Figure 2B**). HTT-D2 was then degraded over time, resulting in a reduction in the levels of red HTT-D2 (**Figure 2C**) and a possible increase of the green HTT-D2 signal, as more fusion protein was newly synthesized. Because a significant decrease was already prominent at 2 h after conversion, the interval for detecting and quantifying the degradation of HTT-D2 was maintained. It is important to note that degradation is not the only process that can occur after conversion of HTT-D2. Converted HTT-D2 could be trafficked and transported along axons, resulting in a decrease in the red signal not due to clearance. However, with the settings employed here and over the short time span of 2 h, no spreading of the red signal was observed, possibly due to the fact that little HTT-D2 was moved from the soma to the axon. Furthermore, converting and imaging a single whole neuronal soma helped exclude the effects of HTT-D2 diffusion within the same neuron, because all cellular compartments were being analyzed simultaneously. To study both diffusion or transport/trafficking it is advisable to obtain fast and higher magnification images and track a smaller and possibly more motile fraction of the protein of interest. It is also important to note that within a set of experiments, each animal represented one biological repeat. Only one neuron per nematode was imaged, each animal was imaged once per session, and imaging occurred over three sessions, which constituted technical repeats. The three sessions required that the animals be synchronized on fresh plates before each experiment either on day 4 or day 10, allowing for whatever environmental variability is imposed on the nematodes. Three sessions also account for any variability arising from the imaging set up (e.g., the laser power varying due to a different temperature between experiments). All biological replicates obtained during the three sessions ($\geq$20 animals) were considered individual samples and utilized to establish statistical significance.

After confirming that both *C. elegans* HTT-D2 strains were effective and establishing the optimal conversion parameters, the differences between the turnover of a disease-causing HTT-D2 protein (i.e., HTTQ97-D2) compared to its physiologically relevant control (HTTQ25-D2) were investigated. First, the degradation of HTT-D2 in different neurons was observed (**Figure 3**). It is known that subtypes of neurons within the nematode´s nervous system vary in their metabolic activity and morphology[21], possibly making a difference in the degradation and rebalancing of the proteome. The neurons of the tail region were compared with those of the head and found to be significantly more active (**Figure 3A**). This finding was only valid for HTTQ25-D2 and not for pathogenic HTTQ97-D2, suggesting that the PN was unable to remove HTT-D2 containing longer glutamine stretches throughout the nervous system (**Figure 3B**).

To further confirm that the model system behaved as expected, conversion experiments were performed over a longer period, allowing the cells' degradation pathways to eliminate the protein of interest almost completely (**Figure 4**). Indeed, there was significantly more degradation of control HTTQ25-D2 24 h after conversion than after 2 h in the head neurons, and extensively more in the tail neurons (**Figure 4A**). Again, the posterior tail neurons more actively removed red HTT-D2, even over an increased timespan. A similar trend was detected for the disease-causing HTTQ97-D2, with a very slight reduction of the red HTT-D2 signal over 24 h. However, HTTQ97-D2 was not removed as readily as HTTQ25-D2, especially after 24 h. It may be

that only the soluble HTTQ97-D2 fraction is efficiently degraded, accounting for the initial diminishing of the red signal and its further mild decrease over time. Importantly, there were two populations of neurons after 24 h: one with a higher degradation rate and one where the red HTT-D2 signal was not degraded at all, or potentially even increased (**Figure 4B**). Increased and stable signal possibly represent already aggregated or continuously aggregating species which were substantially harder to clear from the cells due to their tightly packed amyloid nature. These inclusions, present exclusively when glutamine stretches exceeded the 40 repeat threshold, and which appeared microscopically as foci, have been hypothesized to accumulate as deposits that cannot be easily removed[22]. It is also possible that an increase in the red fluorescent signal was an artifact resulting from technical issues (e.g., use of wrong acquisition parameters, sub-par performance of the microscopy setup, or an erroneous recovery/mounting process). When acquiring images over longer periods of time these variables must be taken into account.

Finally, because neurodegenerative disorders such as HD manifest in adult life, the effect of aging on the rate of HTT-D2 degradation was observed. Conversion experiments were performed in the head and the tail regions of young (day 4) versus old (day 10) nematodes in both HTT-D2 strains (**Figure 5**). For the head neurons, there was no significant change in the rate of degradation due to aging within the lifetime of both HTTQ25-D2 and HTTQ97-D2, possibly because HTT-D2 was removed equally throughout the life of each nematode. However, a very significant change was recorded when comparing old nematodes containing either a pathological or a physiological glutamine stretch. HTTQ97-D2 was not degraded as efficiently as HTTQ25-D2, highlighting the PN´s inability to remove aggregated and possibly toxic species of huntingtin in older nematodes (**Figure 5A**). Again, a more active and significant turnover in the tail neurons was observed. As in the head neurons, a more robust turnover of HTTQ25-D2 was not observed in the tail neurons of young nematodes compared to the older cohort, and degradation was equal at day 4 and day 10. Conversely, significant changes in degradation rates between the control and the pathogenic HTT-D2 strains appeared in young day 4 nematodes, becoming even more significant at day 10. Importantly, tail neurons were able to cope with toxic HTTQ97-D2 in young nematodes, illustrating that various concomitant PN mechanisms might be at work to remove HTT-D2 (**Figure. 5B**). Overall, PN activity diminished over time, possibly due to detrimental effects caused by both aging and the presence of aggregates.

FIGURE AND TABLE LEGENDS:

Figure 1: *C. elegans* expressed huntingtin exon-1 fused to Dendra2 in the nervous system. (**A**) Young, day 4 *C. elegans* pan-neuronally expressing huntingtin exon-1 containing 25 glutamines, fused to Dendra2 in its unconverted green excitation/emission state. Scale bar = 100 µm. Insets show a magnified image of the head (top) and the tail (bottom) neurons. Inset scale bar = 10 µm. (**B**) Young, day 4 *C. elegans* pan-neuronally expressing huntingtin exon-1 containing 97 glutamines, fused to Dendra2 in its unconverted green excitation/emission state. Scale bar = 100 µm. Insets show a magnified image of the tail (top) and the head (bottom) neurons, and the head of a day 7 nematode (far right). Inset scale bar = 10 µm. White arrowheads point to HTTQ97-D2 foci, depicting huntingtin aggregates. (**C**) Channel merge image of HTTQ25-D2 with conversion of the head region. Box represents the portion of the whole *C. elegans* that has been UV irradiated. Scale bar = 100 µm. Inset shows the Dendra2 emission at 488 nm (top, green) and the at 561 nm

(bottom, red). Scale bar = 10 µm. (**D**) Channel merge image of HTTQ97-D2 with conversion of the head region. Scale bar = 100 µm. Box represents the portion of the whole *C. elegans* that has been UV irradiated. Inset shows the Dendra2 emission at 488 nm (top, green) and the at 561 nm (bottom, red). Scale bar = 10 µm.

Figure 2: **Converted red HTT-D2 decreased over time in single neurons.** Tail neurons of HTTQ25-D2. Two neurons are shown simultaneously and independently photoconverted. Images sequentially depict three time points: (**A**) Before irradiation (before), (**B**) immediately after irradiation (conversion), and (**C**) 2 h after irradiation (after). Top panel (green channel) represents HTT-D2 signal collected at 486–553 nm excitation/emission. The white region of interest delineates the neurons that have been irradiated. The middle panel (red channel) shows the converted HTT-D2 signal collected at 580–740 nm excitation/emission. The bottom panel is a merge of the two channels. Scale bar = 5 µm for all images.

Figure 3: **Head and tail neurons exhibited different degradation rates.** Column bar graphs show the percentage of red intensity relative to the initial value at time of conversion (i.e., 100%). Converted red Dendra2 signal decreased overall over the 2 h interval as HTT-D2 was degraded within the neurons of *C. elegans*. Within the nematode's nervous system neuronal subtypes exhibited different degradation rates, with tail neurons showing a more active turnover, but only in nematodes carrying a nonpathogenic polyglutamine stretch. (**A**) Quantification of degradation in HTTQ25-D2 head versus tail neurons. Mean ± SD, unpaired two-tailed Student´s t-test. Numbers are sample/nematodes imaged per region, *P < 0.05. (**B**) Quantification of degradation in HTTQ97-D2 head versus tail neurons. Mean ± SD, unpaired two-tailed Student´s t-test. Numbers are sample/nematodes imaged per region, ns = non-significant.

Figure 4: HTTQ97-D2 was not significantly cleared after 24 h. Column bar graphs show the percentage of red intensity relative to the initial value at time of conversion (i.e., 100%). Converted red Dendra2 signal decreased as HTT-D2 was degraded within the neurons of *C. elegans*. HTT-D2 exhibited different rates of degradation. Even over longer periods of time after conversion, pathogenic HTT-D2 could not be removed compared to its healthy control. (**A**) Quantification of the rate of degradation in HTTQ25-D2 at two time points after conversion (2 h and 24 h) in both head and tail neurons. Mean ± SD, one-way analysis of variance (ANOVA). Numbers are sample/nematodes imaged per time/region, *P < 0.05, ****P < 0.0001. (**B**) Quantification of the rate of degradation in HTTQ97-D2 at two time points after conversion (2 h and 24 h) in both head and tail neurons. Mean ± SD, one-way analysis of variance (ANOVA) followed by Tukey's Multiple Comparison post hoc test. Numbers are sample/nematodes imaged per time/region, ns = non-significant.

Figure 5: Old and young nematodes expressing the pathogenic HTT-D2 did not degrade it efficiently. Column bar graphs show the percentage of red intensity relative to the initial value at time of conversion (i.e., 100%). Converted red Dendra2 signal decreased as HTT-D2 was degraded within the neurons. As the nematode aged, its ability to degrade pathogenic HTT-D2 was additionally impaired throughout its nervous system. (**A**) Quantification of the rate of degradation in the head neurons of young (day 4) and old (day 10) HTTQ25-D2 nematodes

compared to age-matched HTTQ97-D2 nematodes. Mean ± SD, one-way analysis of variance (ANOVA). Numbers are sample/nematodes imaged per strain/day, ****P < 0.0001. (**B**) Rate of degradation 2 h after conversion in the tail neurons of young (day 4) and old (day 10) HTTQ25-D2 nematodes, compared to age-matched HTTQ97-D2 nematodes. Mean ± SD, one-way analysis of variance (ANOVA) followed by Tukey's Multiple Comparison post hoc test. Numbers are sample/nematodes imaged per strain/day, *P < 0.05, ***P < 0.001, ****P < 0.0001.

DISCUSSION:

To comprehend a protein's function it is important to understand its synthesis, location, and degradation. With the development of novel, stable, and bright FPs, visualizing and monitoring POIs has become easier and more efficient. Genetically expressed fusion PAFPs such as Dendra2 are uniquely positioned to study the stability of a POI. Upon exposure to purple-blue light, Dendra2 breaks at a precise location within a triad of conserved amino acids. The fluorophore undergoes a small structural change, resulting in a complete shift of spectra from green to red[23]. This shift allows for the detection and monitoring of any POI linked to Dendra2. Indeed, these fusion constructs were first used to create a *C. elegans* reporter strain to study the ubiquitin-proteasome system in vivo[16]. Dendra2 was also employed to understand the vulnerability of selective neuronal subtypes and their ability to deal with expanded polyglutamine proteins[24], or monitor the induction of autophagy in models of motor neuron disease[25].

A protocol is presented here to monitor in vivo the degradation of huntingtin, a disease-related aggregation-prone protein in a noninvasive manner. After successfully generating a neuronal *C. elegans* model of HD, expressing HTT-D2 pan-neuronally, the rates of degradation of expanded and pathogenic HTT, compared to its physiological counterpart were quantified. Striking differences were observed between neuronal subtypes, between young and aged nematodes, and between the capacity of the PN to deal with toxic glutamine loads over time. This technique can also be applied to follow the location and movement of huntingtin as well as its fate when perturbations to the PN are introduced. siRNA knockdown of key chaperones or administration of compounds that inhibit proteasome activity can uncover the function and importance of these components in aggregation-prone proteins: for example, whether the PN activates specific nodes to compensate for deficiencies[26]. It can also explain the detrimental effects caused by a disease compared to those of normal aging.

Although many different questions can be addressed using this technique, once a desired model has been generated, correct conversion and detection parameters must be established to obtain reliable data. Also crucial is to determine conversion settings that allow for sufficient yield of activated protein without photobleaching or phototoxicity and without undesired conversion. Moreover, for every studied protein within a specific model system, either ex vivo or in vivo, it is necessary to experimentally establish a time period sufficiently large to allow for accurate quantification of the degradation rate.

Dendra2 offers a series of advantages over other PAFPs: 1) it is monomeric and very bright; 2) it has a high contrast photoconversion and a stable photoconverted signal; 3) it can be activated with low phototoxicity by a blue 488 nm laser, which is part of most confocal hardware setups;

4) it efficiently matures at 37 °C for application in mammalian cells; 5) it has no toxic side effects when expressed for extended periods of time[23,27]; and 6) the system is not affected by variations in expression levels between or within an organism or cell, as only the ratio of the Dendra2 signal before and after conversion is quantified. All listed properties make Dendra2 an ideal fluorophore for tracking protein dynamics in real time and monitoring cell fate.

Unfortunately, Dendra2 fusion proteins suffer from some common limitations of fluorescent protein labelling. The construct is a chimeric species often experimentally overexpressed in biological systems, although endogenous expression could be established via genomic engineering. The rate of degradation of Dendra2 itself potentially influences the degradation of the target protein, though it has been described as a highly stable, long-lived protein[27]. Furthermore, Dendra2 is not suitable to track proteins with very fast turnovers as it might not have time for its own proper maturation. Lastly, 405 nm lasers, which are uncommon, are preferred for efficient photoswitching, although they are more toxic to the sample. Indeed, less phototoxic blue light can be utilized to both visualize green Dendra2 and convert it when laser power is at high intensity. This particular feature should always be kept in mind, as prolonged exposure will produce unwanted conversion and potentially wrong measurements. Finally, it may be problematic to use Dendra2 in combination with green or red fluorophores. However, many different PAFPs are available to investigate the dynamics of several proteins simultaneously.

Experiments utilizing Dendra2 and other PAFPs have been linked to fluorescence recovery after photobleaching (FRAP) and radioactive pulse-chase labelling techniques. In a FRAP setting it is impossible to distinguish proteins re-entering an ROI from newly formed fluorescent protein, and constant monitoring and visualization of the sample is necessary. With Dendra2, two clearly distinguishable populations are generated that can be independently observed over time so the replaced and newly synthetized "inactive" form of green Dendra2 can be tracked and quantified[16]. Dendra2 is also a useful probe in super resolution microscopy such as total internal reflection fluorescent microscopy (TIRF)[28] and photoactivation localization microscopy (PALM)[29]. In the near future such advancements will allow for better localization and potentially single molecule tracking of any POI, allowing to uncover more subtle differences within and between samples and ultimately yielding new information on the life and fate of any POI within a biological system.

ACKNOWLEDGMENTS:
We acknowledge the DFG (KI-1988/5-1 to JK, NeuroCure PhD fellowship by the NeuroCure Cluster of Excellence to MLP) for funding. We also acknowledge the Imaging Core Facility of the Leibniz Research Institute for Molecular Pharmacology Berlin (FMP) for providing the imaging set up. In addition, we would like to thank Diogo Feleciano who established the Dendra2 system in the lab and provided instructions.

DISCLOSURES:
The authors have nothing to disclose.

REFERENCES:

1. Tsien, R. Y. the Green Fluorescent Protein. *Annual Review of Biochemistry.* **67** (1), 509–544 (1998).
2. Lippincott-Schwartz, J., Patterson, G. H. Fluorescent Proteins for Photoactivation Experiments. *Methods in Cell Biology.* **85** (08), 45–61 (2008).
3. Lukyanov, K. A., Chudakov, D. M., Lukyanov, S., Verkhusha, V. V. Photoactivatable fluorescent proteins. *Nature Reviews Molecular Cell Biology.* **6** (11), 885–890 (2005).
4. Chudakov, D. M., Lukyanov, S., Lukyanov, K. A. Tracking intracellular protein movements using photoswitchable fluorescent proteins PS-CFP2 and Dendra2. *Nature Protocols.* **2** (8), 2024–2032 (2007).
5. Gurskaya, N. G. et al. Engineering of a monomeric green-to-red photoactivatable fluorescent protein induced by blue light. *Nature Biotechnology.* **24** (4), 461–465 (2006).
6. Chudakov, D. M., Lukyanov, S., Lukyanov, K. A. Using photoactivatable fluorescent protein Dendra2 to track protein movement. *BioTechniques.* **42** (5), 553–565 (2007).
7. Bates, G. P. et al. Huntington disease. *Nature Reviews Disease Primers.* **1** (1), 15005 (2015).
8. Nussbaum-Krammer, C. I., Morimoto, R. I. Caenorhabditis elegans as a model system for studying non-cellautonomous mechanisms in protein-misfolding diseases. *DMM Disease Models and Mechanisms.* **7** (1), 31–39 (2014).
9. Chen, L., Fu, Y., Ren, M., Xiao, B., Rubin, C. S. A RasGRP, C. elegans RGEF-1b, Couples External Stimuli to Behavior by Activating LET-60 (Ras) in Sensory Neurons. *Neuron.* **70** (1), 51–65 (2011).
10. Addgene. Plasmids 101: A Desktop Resource (3rd Edition), 45-50, www.addgene.org (2017).
11. Gibson, D. G. et al. Enzymatic assembly of DNA molecules up to several hundred kilobases. *Nature Methods.* **6** (5), 343–345 (2009).
12. Mello, C. C., Kramer, J. M., Stinchcomb, D., Ambros, V. Efficient gene transfer in C.elegans: extrachromosomal maintenance and integration of transforming sequences. *The EMBO Journal.* **10** (12), 3959–3970 (1991).
13. Mariol, M. C., Walter, L., Bellemin, S., Gieseler, K. A rapid protocol for integrating extrachromosomal arrays with high transmission rate into the C. elegans genome. *Journal of Visualized Experiments.* 82, e50773 (2013).
14. Kreis, P. et al. ATM phosphorylation of the actin-binding protein drebrin controls oxidation stress-resistance in mammalian neurons and C. elegans. *Nature Communications.* **10** (1), 1–13 (2019).
15. Juenemann, K., Wiemhoefer, A., Reits, E. A. Detection of ubiquitinated huntingtin species in intracellular aggregates. *Frontiers in Molecular Neuroscience.* **8**, Jan 1–8 (2015).
16. Hamer, G., Matilainen, O., Holmberg, C. I. A photoconvertible reporter of the ubiquitin-proteasome system i*n vivo*. *Nature Methods.* **7** (6), 473–478 (2010).
17. Porta-de-la-Riva, M., Fontrodona, L., Villanueva, A., Cerón, J. Basic Caenorhabditis elegans methods: Synchronization and observation. *Journal of Visualized Experiments.* 64, e4019 (2012).
18. Stiernagle, T. Maintenance of C. elegans. *WormBook : the online review of C. elegans biology.* 1999, 1–11 (2006).
19. Collins, J. J., Huang, C., Hughes, S., Kornfeld, K. The measurement and analysis of age-related changes in Caenorhabditis elegans. *WormBook : the online review of C. elegans biology.*

1–21 (2008).
20. Schindelin, J. et al. Fiji: An open-source platform for biological-image analysis. *Nature Methods.* **9** (7), 676–682 (2012).
21. Hobert, O. Specification of the nervous system. *WormBook* 1–19 (2005).
22. Ross, C. A., Poirier, M. A. What is the role of protein aggregation in neurodegeneration? *Nature Reviews Molecular Cell Biology.* **6** (11), 891–898 (2005).
23. Adam, V., Nienhaus, K., Bourgeois, D., Nienhaus, G. U. Structural basis of enhanced photoconversion yield in green fluorescent protein-like protein Dendra2. *Biochemistry.* **48** (22), 4905–4915 (2009).
24. Tsvetkov, A. S. et al. Proteostasis of polyglutamine varies among neurons and predicts neurodegeneration. *Nature Chemical Biology* **9** (9), 586–594 (2013).
25. Barmada, S. J. et al. Autophagy induction enhances TDP43 turnover and survival in neuronal ALS models. *Nature Chemical Biology.* **10** (8), 677–685 (2014).
26. Feleciano, D. R. et al. Crosstalk Between Chaperone-Mediated Protein Disaggregation and Proteolytic Pathways in Aging and Disease. *Frontiers in Aging Neuroscience.* **11**, Jan (2019).
27. Zhang, L. et al. Method for real-time monitoring of protein degradation at the single cell level. *BioTechniques.* **42** (4), 446–450 (2007).
28. Zhang, Z., Heidary, D. K., Richards, C. I. High resolution measurement of membrane receptor endocytosis. *Journal of Biological Methods.* **5** (4), 105 (2018).
29. Gunewardene, M. S. et al. Superresolution imaging of multiple fluorescent proteins with highly overlapping emission spectra in living cells. *Biophysical Journal.* **101** (6), 1522–1528 (2011).

Figure 1

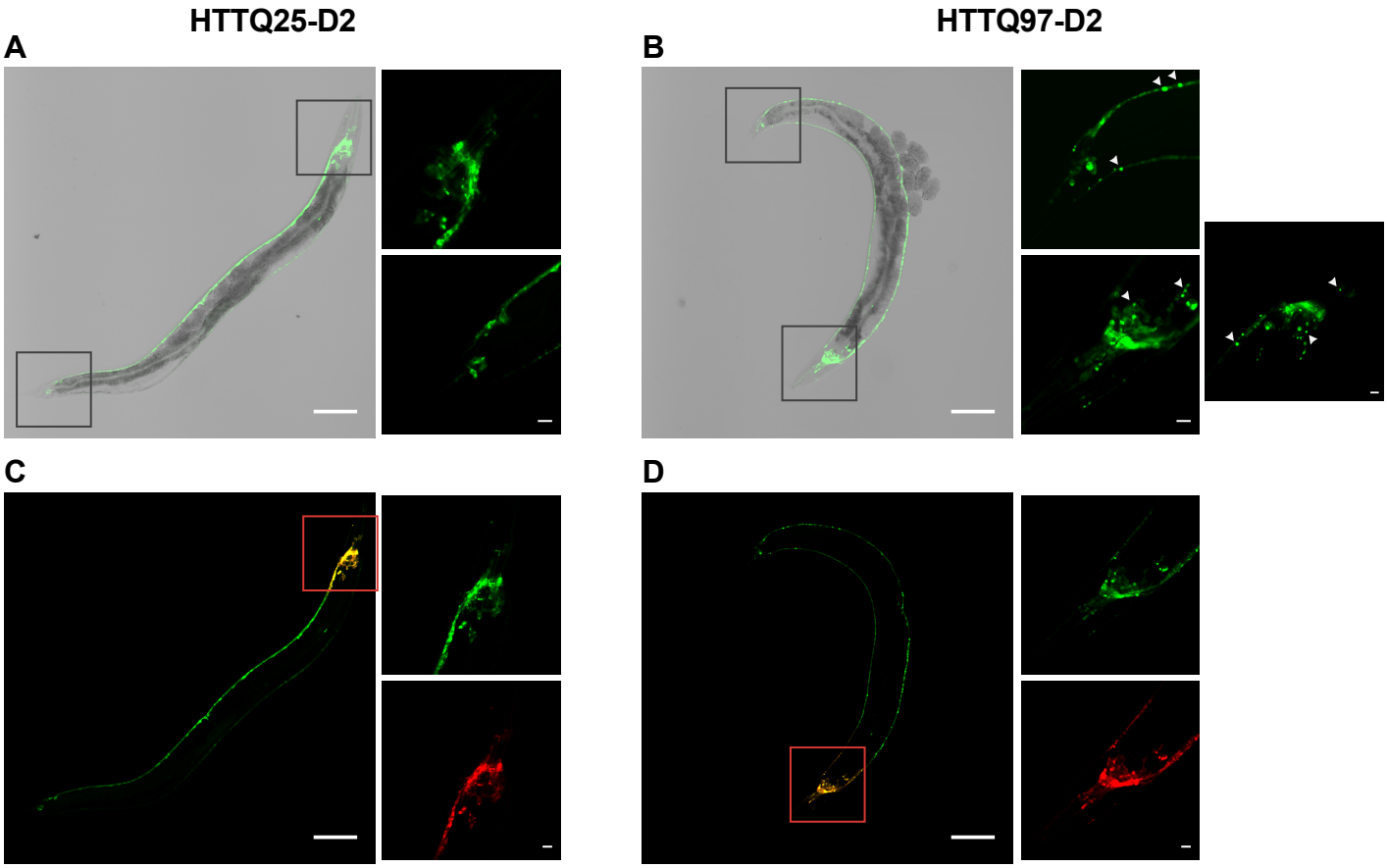

Figure 2

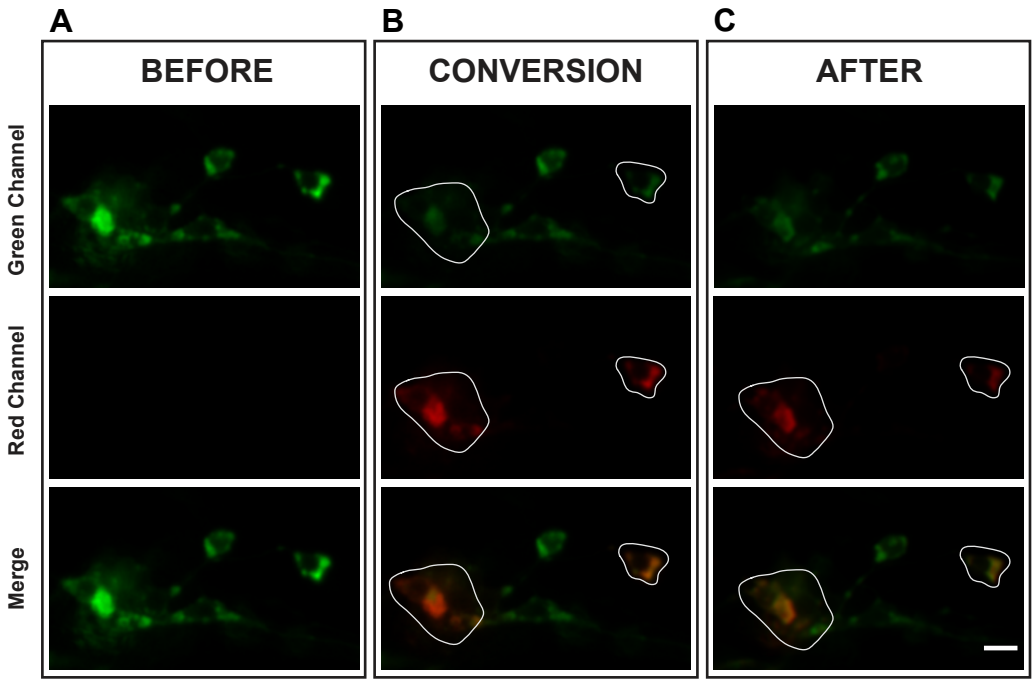

Figure 3

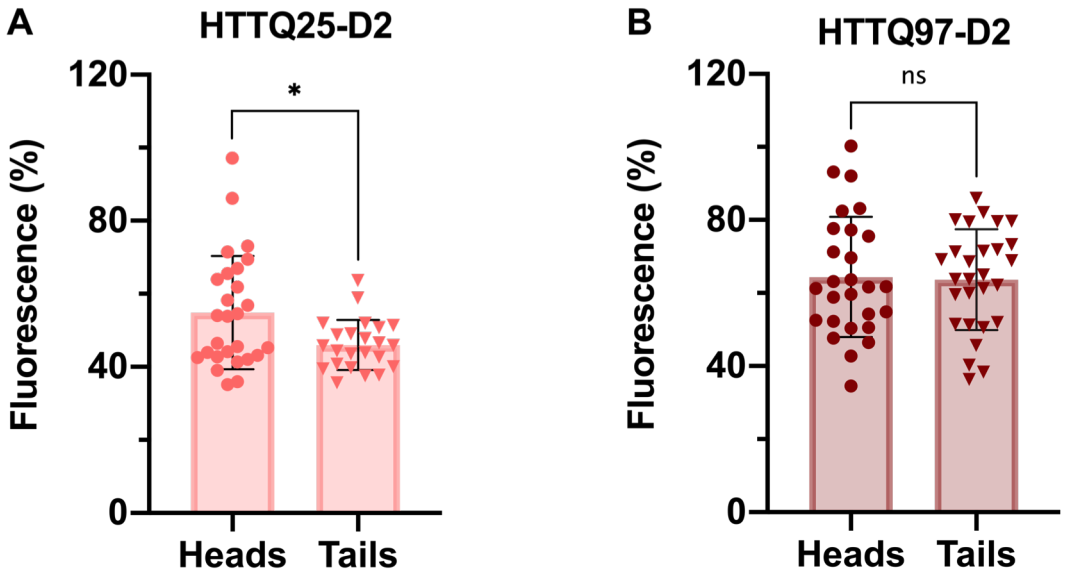

Figure 4

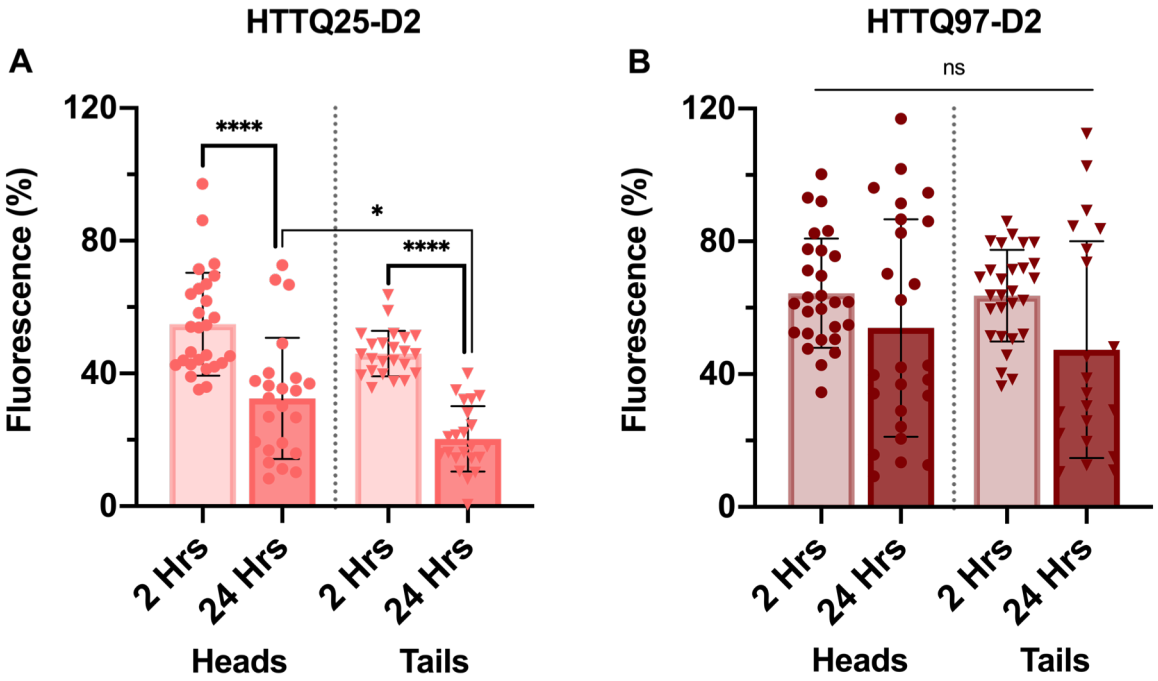

Figure 5

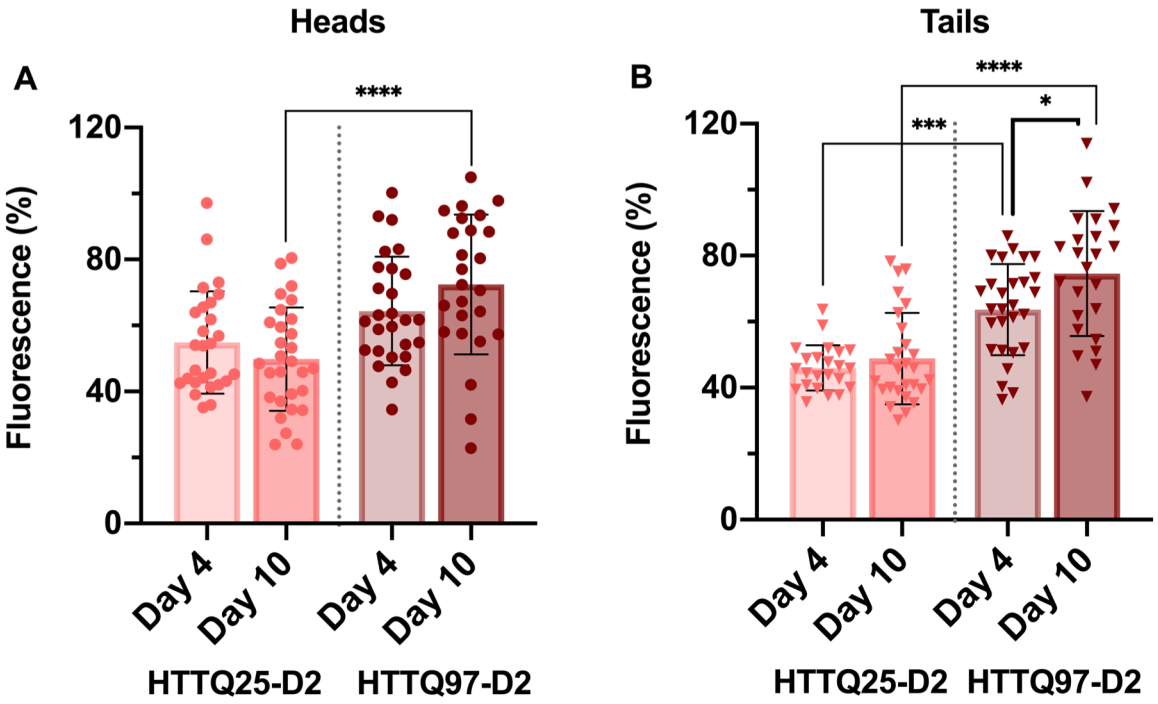

Materials

Click here to access/download;Table of Materials;JoVE_Dendra2_Table_of_Materials.xlsx

Name of Material/Equipment	Company	Catalog Number
Agar-Agar Kobe I	Carl Roth GmbH + Co. KG	5210.2
Agarose, Universal Grade	Bio & Sell GmbH	BS20.46.500
BD Bacto Peptone	BD-Bionsciences	211677
Deckgläser-18x18mm	Carl Roth GmbH + Co. KG	0657.2
EC Plan-Neufluar 20x/0.50 Ph2 M27	Carl Zeiss AG	
Fiji/ImageJ 1.52p	NIH	
Levamisole Hydrochloride	AppliChem GmbH	A4341
LSM710-ConfoCor3	Carl Zeiss AG	
Mounting stereomicroscope	Leica Camera AG	
neuronal-HTTQ25-Dendra2	this paper	
neuronal-HTTQ97-Dendra2	this paper	
OP50 Escherichia coli	CAENORHABDITIS GENETICS CENTER (CGC)	OP50
Sodium Chloride	Carl Roth GmbH + Co. KG	3957.2
Standard-Objektträger	Carl Roth GmbH + Co. KG	0656.1
ZEN2010 B SP1	Carl Zeiss AG	

Comments/Description
NGM component
Mounting slide component
NGM component
Cover slips
Objective
Analysis Software
Anesthetic
Laser Scanning Confocal Micoscope
Mounting microscope
C. elegans strain
C. elegans strain
Nematode food source
NGM component
Glass slides
Confocal acquisition software

Rebuttal letter for:

In vivo quantification of protein turnover in aging *C. elegans* using the photoconvertable Denrdra2

We would like to thank both reviewers for their time to review our manuscript and for the constructive criticism that allowed us to edit and improve the revised manuscript. Below we will comment on each specific point of both reviewers and we highlight our response in red for clarity.

Reviewer #1:
Manuscript Summary:
In this manuscript, Pigazzini et al provide a comprehensive protocol for measuring the turnover of Dendra2-tagged proteins in C. elegans. The method allows tracking the metabolism of a protein in living organisms, in whatever cell type designated, and is inherently powerful and tractable. In particular, the use of C. elegans is outstanding, allowing in-depth investigations of pathways and factors involved in the degradation of the protein in question. The final manuscript should be very helpful for any wishing to replicate these experiments. However, the current version has several grammatical errors and oversights, and could be improved by attention to the following concerns:

We thank the reviewer for the overall positive feedback and the constructive criticism.

Major concerns
The authors fail to acknowledge the use of Dendra2 for labeling and tracking the metabolism of HTT and other neurodegenerative disease-associated proteins in previous studies. (PMID: 23873212, PMID: 24974230, PMID: 31018129, PMID: 30015619)

We thank the reviewer for pointing out missing references. Yet, we have referenced Tsvetkov et al., 2013 (PMID: 23873212; our reference number 19) as it is an elegant demonstration of the power of the technique *ex vivo* for aggregation-prone proteins. We did not intentionally exclude references, but also do not think that including all publications that utilized Dendra2 so far to study protein aggregation and neurodegeneration adds any further information.

The authors also fail to acknowledge previous studies confirming that Dendra2 labeling does not affect the turnover of target proteins such as HTT, and that the half-life of HTT-D2 as measured by fluorescence microscopy is similar to that of HTT as determined by traditional metabolic pulse chase. This is an important question that many readers may have when reading the proposal.

The reviewer´s observations are very valuable. We refer to a series of papers in which various proteins of interest were tagged with Dendra2 and their turnover measured. Hamer et al., (2011), performed control experiments in *C. elegans* demonstrating that Dendra2 is stable over long periods of time and only with the addition of a selected POI gets degraded at various

rates. Zhang et al., (2007), also performed extensive measurements in HEK293 cells on both the stability of unconverted green Dendra2 and the high stability of converted red Dendra2, and state that "practically no decay of red fluorescence after Dendra2 photoconversion was observed". Only with the addition of a selected protein, Dendra2 is degraded at a rapid rate. In agreement with these publications, in our HTT-D2 system, we observe that degradation already occurs within a few hours after conversion. It would be interesting to compare the overall degradation rate of HTT-D2 compared to other huntingtin-expressing system, however this is not a goal of this experimental set. The nematode does not have an endogenous homologue of huntingtin and the protein is completely foreign to this environment; we cannot be sure therefore that the results would be comparable. Our main aim is to show that Dendra2 can be used as a marker for degradation when fused to a disease-relevant protein and that some properties of the disease-relevant proteins (for example the effects of an expanded glutamine stretch), can have visible repercussions on its degradation. Further experiments to identify which components of the degradation machineries or upstream signalling pathways are involved can then also be studied.

The authors should also the discuss how photo conversion of Dendra2 at 488nm (the excitation wavelength for non-photoconverted Dendra2; PMID: 17515192) during the data acquisition period (step 7) may affect half-life calculations, and how this can be avoided.

We thank the reviewer for this comment: it is indeed important not to expose Dendra2 to 488 laser light for prolonged time or intensity to avoid it´s conversion. We state this at two points in the manuscript: in section 6.3 as an important point (line 198), and again in the discussion (from line 486), where we mention that conversion can occur at 488 nm when the intensity or exposure time is long enough. However, this property is not necessarily a disadvantage as many microscopes are not equipped with a 405 laser, while 488 lasers are very common, allowing for the experiment to still be performed - with some care. We also thank the reviewer for the suggested reference that was however already included in the manuscript.

Section 8.6 - integrated density measurements are highly dependent on area, which can potentially confound measurements. For instance, larger ROIs will have larger integrated densities. Mean intensity corrects for area and may be a more appropriate measure if the protein is distributed diffusely.

We decided to use the RawIntDen as we want to obtain a measurement between time points of the same neuron, which would have the same area/volume. We therefore want the sum of the values in our selection, and not its mean, which is dependent on area. Especially after 2 hours, as the nematode is immobile, the location/size/shape of the single imaged neuron is very similar, allowing to draw a comparable ROI. Furthermore, because the pinhole is set to the maximum, the confocal plane imaged is large enough to acquire fluorescence from the whole neuron and the resulting scan should include the intensity of the whole neuronal area. As for comparison between neurons/nematodes, the percentage of degradation are calculated within the same neuron and the final ratio is independent of the cell size.

Section 9.3 - some discussion of replicates is required. For example, are individual neurons from the same animal considered technical replicates, while those from different animals are biological replicates? How are these values combined to allow for statistical comparisons?

We agree that some clarifications might be useful: each animal represents a biological repeat. Only one neuron is imaged per animal, each animal is imaged once per session, and imaging occurs over three session, which constitute technical repeats. The three session require that animals are synchronised on fresh plates before each experiment either on day 4 or day 10, allowing for whatever environmental variability is imposed on the nematodes. Three session also account for any variability that arises from the imaging set-up (e.g. laser power not exactly the same due to the room´s different temperature). All biological replicates obtained during the three repeats are then considered individual samples and utilised (i.e. N=20 nematodes) to establish significance.

line 329: is the expression of HTT-D2 different in head vs. tail regions? Does expression or abundance of HTT-D2 affect its degradation? These questions should be answered before concluding that the metabolism of HTT-D2 differs between cell types.

The expression does not seem to change between head and tail of the same strain. Chen et al. (2011) previously described a robust expression of a GFP fusion protein under the control of *rgef-1* promoter over time and throughout the nervous system, but we have not quantified this experimentally ourselves. As the transgene is not integrated within the nematode's genome, the expression HTT-D2 can vary between animals. However, we only measure the difference of the converted red Dendra2 between two time points, and we observe that within this time span the signal decreases. Furthermore, most likely green HTT-D2 is constantly being removed and degraded, and re-synthetized, but its total abundance, or clearance, is not relevant to and cannot interfere with our measurements. The presence of other HTT-D2 within the cell should not have an effect on its turnover, as Dendra2 itself for example is very stable. We conclude that the increased degradation rate is due to either the protein being more easily degraded (e.g. when HTT has 25Qs rather than 97Qs) or when the metabolism of a cells is more active.

line 344: is the expression of HTT25Q-D2 the same as HTT97Q-D2? Is the photoconversion as efficient? For example, is the absolute red fluorescence the same after conversion of HTT25Q-D2 and HTT97Q-D2?

As mentioned above, we have not established quantitatively (e.g. via RT-qPCR or western blot quantification at different time points) if the expression is the same between the strains. However, we are measuring the difference between a relative and not an absolute value.
We do not fully convert HTT-D2 of a single neuron, but just a fraction. We then establish the ratio of degradation: not all red HTT-D2 is removed within our time points. It is important to state, and this is stressed in the protocol, that the settings used to perform the conversion are exactly the same throughout all experiments (e.g. laser power, iteration number, pinhole size, pixel dwell, etc). Although we expect some degree of variation imposed by both the set-up and the nematode´s biology, we can also assume that the conversion is occurring similarly within various neurons of different animals.

line 372: does the exogenous transgene continue to overexpress protein over time? It could be that the cells accumulate higher and higher amounts of protein as they age. To determine this, the authors could measure GFP fluorescence as a function of age.

The exogenous gene is expressed over time controlled by the *rgef-1* promoter, as referenced in Chen et al. (2011). But even in the presence of higher amounts of protein, only the relative converted red HTT-D2, and its consequential degradation, is measured to establish the rate at which neurons degrade HTT-D2. Newly synthesized HTT-D2 would be in its non-converted green state and thus not be considered for the analysis.

Figure 4B - Also, the large degree of variability in HTT97Q-D2 expressing cells is unusual. It looks like at the 24H time point there are really two populations of neurons, those which have around 40% of fluorescence and those with little or no decrease in fluorescence. Does aggregation correlate with this? For example, is there higher % fluorescence in cells displaying HT97Q-D2 aggregates? In general, this is an important point which can affect all of the authors measurements of degradation; that is, whether or not aggregation itself affects measurements of protein degradation. It could be that this method is not accurate for measuring the turnover of aggregate-prone proteins, as alluded to in previous work (PMID: 23873212, PMID: 24974230)

We appreciate the reviewer´s comment and agree that there are 2 populations present at 24 hours after conversion, and, as the reviewer points out, one of these populations resembles aggregated species. The fluorescence here is not necessarily higher, but the location/shape of HTT-D2 appears as condensed foci rather than diffused protein. It is possible that some of the mutant form of HTT-D2 has incorporated into higher amyloid structure over longer period of time and escaped its degradation. Aggregation most likely affects protein degradation and we believe the technique can still be used for aggregation-prone protein, but care has to be taken. For example, it is possible to distinguish the rate of degradation when measuring HTT-D2 exclusively in its soluble form. It is also possible to investigate the aggregates themselves, by converting HTT-D2 foci specifically, for example in different neurons or at different ages of the nematode. Such experiment would provide insight on the nature of the aggregate itself: can smaller aggregates be cleared faster? Do different neurons exhibit different degradation rates? And finally, what is the fate of both, the aggregates and the soluble HTT-D2, when the system is perturbed, for example by knockdown of specific chaperone or proteolytic pathways. We strongly believe the method can be employed to study aggregation, yet we agree with the reviewer, care must be taken when designing the experiment.

Minor concerns

p.1 line 26: "…how to track the disease-causing protein huntingtin" should be "…how to track the degradation of the disease-causing protein huntingtin."

We thank the reviewer for this improved phrasing and have amended the text accordingly.

p.1 line 36: "…machineries controlling degradation are deficient in the presence of aggregated huntingtin…" this makes it seem as if the pathway is compromised, rather than slow turnover of the aggregated protein itself (only the latter can be measured by Dendra2 labeling).

It has been shown that amyloid proteins can affect the activity of one major protein clearance pathway, the ubiquitin proteasome (UPS) in their fibrilized state (Hipp et al., 2012 JCB), but also as soluble oligomeric species (Thibaudeau et al., 2018 NatComm). As we cannot exclude that the presence of mutant huntingtin already in its soluble form is contributing to the impairment of the proteostasis network, we have rephrased the sentence to "machineries controlling degradation are deficient in the presence of *mutant* huntingtin…".

p. 1 line 37: huntingtin should not be capitalized

We apologise for this oversight and have amended the text.

p. 1 line 37: "… cease with the progression of aging" — this statement is confusing, unclear what the authors are trying to say

With the sentence we would like to stress that during aging the effect of huntingtin on the proteostasis network is aggravated. We have amended the text to make the statement more clear.

p.1 line 40: "and the proteases…" should be "and the proteases responsible for its degradation…"

We thank the author for pointing this out and have amended the sentence for clarity.

p.1 line 41: "…further biological processes." This statement is vague

We apologise for the vagueness and have removed the end of the sentence.

p.2 line 48: discussion of timer proteins is not fully fleshed out, more confusing than informative here

We have omitted the concept as indeed it is not the scope of this protocol to discuss timer proteins.

p.2 line 58: "for organelles:" colon is out of place, and this sentence is awkward as written

We agree about the unfortunate wording and have changed our sentence.

p.2 line 69: huntingtin should not be capitalized

We apologise for this oversight and have amended the text.

p. 2 line 75: "mutated" is not used correctly here. The mutation is the CAG expansion in the gene encoding HTT.

We apologise for our terminology: indeed the gene is mutated, resulting in a mutant protein.

p. 2 line 82: it is unclear from this discussion whether C. elegans have a native HTT promoter driving HTT-D2, or the authors are using a transgene for pan-neuronal expression.

We apologise for the confusion. HTT-D2 is overexpressed as a transgene and remains extra-chromosomally within the nematode. It is stated in more detail as a first step on how to generate the Dendra2 construct (section 1) for *C. elegans* expression. We have however amended the introduction text to state the nature of the transgene.

p.3 line 93: "only but a few information…" this sentence is awkward and not grammatically correct

We thank the reviewer for pointing this out. We have changed the text to state observations, rather than information.

Section 7.3 - how can autofluorescence be distinguished from red (photo converted) Dendra2 fluorescence?

We thank the author for pointing out this. Autofluorescence will be visible under all fluorescent light, without the use of laser power, and not necessarily only in the red channel. However, during laser scanning, both red and green Dendra2 will appear as a low/weak signal. We have amended the statement in the text to be clearer.

Section 8.8 - low signal intensity in the red channel may preclude drawing an accurate ROI around the photo converted neuron. Using the green channel for ROI generation might be easier.

We agree with the reviewer and added a note to suggest this, however, it should still be possible to identify the contours of the converted neuron by using the thresholding function in the red channel.

Section 9.1 - is there any measurement to confirm the degree or magnitude of photo conversion?

The degree/magnitude of conversion could possibly be established by calculating the decrease in the green Dendra2. An intensity image of the green Dendra2 would need to be obtained before conversion and then right after conversion. A ratio could then be calculated between these two, describing how much Dendra2 has been converted. However, since we do not focus on how much Dendra2 is converted overall, but on how much is removed of the converted species, we did not embark in obtaining these calculations.

line 305: "…pathogenic repeat with 97 glutamine residues"

We included the missing terminology.

line 348: it may be difficult to measure protein degradation in the setting of aggregation, since this can lead to paradoxical increases in red (photo converted) fluorescence intensity

We agree with the reviewer´s statement that the red signal could increase upon aggregation. However, we would like to point out that we measure the degradation mostly after 2 hours after conversion. In such a short time span it is unlikely that HTT-D2 incorporated into aggregates. In addition, we also convert HTT-D2 within a complete single neuron, rather than specific foci. Thus, we measure the red Dendra2 fluorescence of the entire cell, minimising the risk of artefacts.

Figure 1A/B - Labeling the panels themselves with HTT25Q-D2 (A) or HTT97Q-D2 (B) would be helpful.

The reviewer is right and we have added the title to the panels for clarity.

Figure 1A/B - Also, the differences between HTT25Q-D2 and HTT97Q-D2 are not very evident from these images; small foci look to be evident in HTT25Q-D2 expressing animals as well as those expressing HTT97Q-D2

The selected nematodes expressing HTT25Q-D2 and HTTQ97-D2 are young and foci formation is much more prominent as the nematode ages. The foci can be distinguished by intensity measurements, size and shape.

Figure 1A/B - Also, it would be helpful to see the red channel pre photo conversion, to compare with C/D.

The aim of the image depicted in figure 1 is to show that a specific ROI can be converted and that the green Dendra2 is not wholly converted, but colocalises with the converted red Dendra2. A pre-conversion image of the red channel is completely black and not very informative. Yet, we have included the red channel pre-conversion in figure 2, where all the conversion steps appear.

Figure 2 - it would be helpful show ROI used to photocovert Dendra2

We thank the reviewer for the suggestion and have included the ROI used to convert the single neurons.

Figure 3A - differences here appear to be due to 2 outliers in the head neurons. Is the comparison the same when these two outliers are removed?

Yes, the significance is still present even after the outliers have been removed. Outliers were identified in PRISM8 software using the Identify Outliers function set with ROUT method to Q=5%.

Figure 3A/B - how many animals (not just neurons) were used for these calculations? This should be included for all plots in Figure 3, 4 and 5

The number of neurons equals the number of animals as a single neuron was converted from each nematode. We have previously stated the n number in the figure legend, but have included the n number within the graph of figure 3 in the revised manuscript.

Figure 3 - in general, it would be better if A and B were plotted on one plot and an ANOVA used (instead of two students T-tests)

The reason for choosing the students T-test was to statistically evaluate the rate of degradation within different neurons of the same strain.

Figure 4B - in some cases, fluorescence increases with time… the authors may want to comment on this.

We postulate that either the acquisition parameters were not maintained appropriately, the system performed sub-par on the second day of acquisition, or another step in the recovery/mounting procedure was not correct. These are only suppositions, but indeed this event is only visible 24 hours after conversion. These possibilities have now been included in the manuscript in the section discussing the results (line 586).

Figure 4 legend - line 414: "…HTT-D2 exhibit different rates of conversion" should be "HTT-D2 exhibit different rates of degradation" (hopefully)

We thank the reviewer for pointing out this oversight, it is indeed degradation.

Figure 5 - in this and all figures with statistics, please list the ANOVA post-test used to determine significance

We have included the missing information in the revised manuscript.

Figure 5 legend - The title has a typo in it. Also, please comment on how many hours after photoconversion measurements are taken.

We apologise for our oversight and have corrected the legend, including adding the time after conversion. The samples were measured 120 minutes after conversion.

The authors should also mention that prolonged exposure to low-wavelength light (used to photo convert Dendra2) can elicit phototoxicity. In addition, citations are sometimes missing from the text where they would otherwise be expected; for instance, line 472-473.

We have stressed the ability of blue light to also convert Dendra2. We have added several 'warnings' and references as suggested.

Reviewer #2:
Manuscript Summary:
This manuscript provides a thorough and clear protocol for using Dendra2-labeled proteins in C. elegans to quantify protein degradation. The manuscript and video would provide a useful protocol for labs that are new to photo-activatable fluorescent protein analysis. I have a few concerns that I think should be addressed before publication, but these should not require any new experiments and can hopefully be addressed relatively quickly.

We thank the reviewer for the positive assessment of our manuscript and thank the reviewer for the constructive criticism.

Major Concerns:
1. Figure 4 and Figure 5 need a more careful consideration of which statistical analysis to use, particularly if this protocol is to be a guideline for other labs. Because two factors are considered (head vs tail and 2h vs 24h, or Q25 vs Q97 and 4d vs 10d), a 2-way ANOVA (or other statistical model considering multiple factors) would be more appropriate than a 1-way ANOVA. If data points from the same worm are included at different time points, then a repeated-measures test would also be more appropriate. Finally, the type of pairwise comparisons and multiple testing corrections need to be defined clearly in the text.

We thank the reviewer for this comment. We have indicated in the text which type of post hoc comparison test was used. Our aim is to describe a protocol on how to create a system to track degradation, how to acquire data and analyse the resulting images, while the final statistical evaluation is chosen by the end users according to their hypothesis.
We have selected a 1-way ANOVA as the comparison considers one independent variable at each point even though more groups are compared. For example, in figure 4, we compare the heads at time 2 hours vs time 24 hours of the HTTQ25-D2 strain, or the difference between heads and tails at time 2 hours only. We do not for example compare the 'head values' at 2

hours to the tail values at 24 hours. A similar analysis was performed for figure 5. We concede the graphical representation we have used might be a personal preference and the data can actually be grouped and used to compare multiple parameters at the same time, or also just two, for which a T-test would probably suffice. For this data, applying a two-way ANOVA did not change the statistical significance results.

2. While the data in Figures 3-5 show clear differences between groups in many cases, there is a large variance in data among different worms. The manuscript would benefit from a short discussion of the expected variance within groups, and the predicted n numbers needed for labs to reproduce these results (or to find more subtle differences between groups).

The reviewer is correct in outlining the variation between *C. elegans* nematodes. Although they are supposed to be isogenic, many environmental factors impact their development and maintenance and consequently their protein expression, and indeed results can be variable also between different labs. It is common in the community to perform imaging on an average of 20 nematodes (each nematode, rather than a single neuron imaged, being n=1), and we would also suggest to continue with this number in three biological repeats. Regarding the very subtle differences, the technique can potentially be improved. For example, a z-stack of the single neurons can be acquired instead of a single plane with open pinhole, and the intensity measured from the maximum projection of the stack; acquisition might however require a spinning-disk confocal rather than a normal laser scanning, as the prolonged exposure to blue light will convert newly synthetized Dendra2 and skew the measurement of pre-converted red Dendra2. Another improvement could be the targeting of the exact same neuron in all samples: an easier way to achieve this is to select a promoter that exclusively drives expression of Dendra2 in a specific neuron, rather than pan-neuronally. Although the subtle differences imposed by the POI within that neuronal class might be detected, other characteristics of the protein itself or the cellular environment might be lost.

3. In principle, a decrease in local signal for converted red-Dendra2 could result from either degradation of the protein or its diffusion and/or transport to a different cellular component (e.g. axons or dendrites). A short discussion of this limitation, and/or potential ways this protocol can get around this limitation, would be useful.

The reviewer raises an interesting issue. The decrease in Dendra2 could be due to transport and/or diffusion and indeed one of the advantages of the system is the ability to track the tagged POI. To trace transport along a specific axon or observe diffusion it would be better to convert a small fraction of Dendra2, and follow this process at high speed and magnification. For our application, we convert a whole single neuronal soma, at relatively low magnification (20x) and monitor the same cell over longer time. We assume that HTT-D2 remains largely in the neuronal soma and only very little amount is transported to the axons, as we do not observe a 'spreading' of the red signal. We included this issue in the revised manuscript, in the results section (from line 552).

4. For the steps requiring manual selection of regions of interest (steps 6.4 and 8.5), it will be important to include either figures or clear video demonstrations of how to properly select these regions manually.

The selection of the ROIs is paramount to the technique and analysis, and we do believe this is the reason why a visual presentation in a JoVE format is suited very well. With the video explanation we can clearly show screenshots of the process of acquisition on the microscope set-up and of analysis with the Fiji software.

Minor Concerns:
1. The description in Lines 354-364 is somewhat unclear in describing the results of Figure 5. A simpler and more explicit description of each comparison might help here.

We thank the reviewer for the advice and have modified the text to provide a clearer explanation.

2. The legend for Figure 3 should state the time point after conversion for the data represented here.

We have modified the legend accordingly.